Biology 555
Nucleic Acid Structure
B. Stark

I. DNA double helical forms
- >> forces stabilizing double helices
  - > H-bonds
  - > stacking forces
    - > hydrophobic forces
    - > van der Waals (London dispersion) forces
- >> B-DNA (most or all naturally occurring DNA is B-form)
- >> A-DNA
  - > general features/average properties
  - > RNA-DNA hybrids are also A form
- >> Z-DNA
  - > general features/average properties
- >> other forms
  - > general features/average properties

II. B-DNA
- >> average parameters
- >> microheterogeneity
  - > base to base
  - > within a base pair

III. RNA
- >> forces stabilizing double helices
  - > H-bonds
  - > stacking forces
    - > hydrophobic forces
    - > van der Waals (London dispersion) forces
- >> RNA molecules are simultaneously both single and double stranded
- >> RNA double helical regions are A-form
- >> 3D structures involve both "typical" and unusual base pairs
- >> yeast phenylalanyl tRNA as an example
- >> "pseudoknots" are important structures in many RNAs, including catalytic RNAs ("ribozymes")

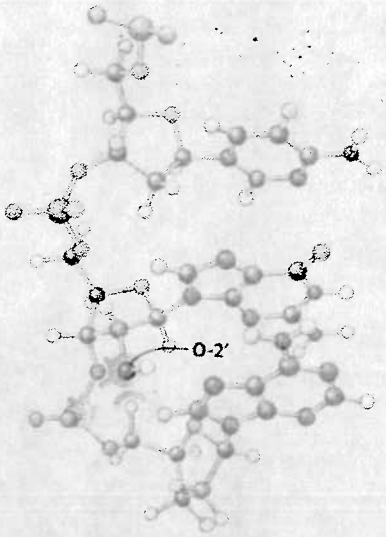

FIGURE 27.6 Steric clash. The introduction of a 2′-hydroxyl group into a B-form structure leads to several steric clashes with nearby atoms.

plane (a conformation called C-2′-endo). The C-3′-endo puckering in A-DNA leads to a 19-degree tilting of the base pairs away from the normal to the helix. The phosphates and other groups in the A helix bind fewer H_2O molecules than do those in B-DNA. Hence, dehydration favors the A form.

The A helix is not confined to dehydrated DNA. *Double-stranded regions of RNA and at least some RNA–DNA hybrids adopt a double-helical form very similar to that of A-DNA.* The position of the 2′-hydroxyl group of ribose prevents RNA from forming a classic Watson-Crick B helix because of steric hindrance (Figure 27.6): the 2′-oxygen atom would come too close to three atoms of the adjoining phosphate group and one atom in the next base. In an A-type helix, in contrast, the 2′-oxygen projects outward, away from other atoms.

27.1.2 The Major and Minor Grooves Are Lined by Sequence-Specific Hydrogen-Bonding Groups

Double-helical nucleic acid molecules contain two grooves, called the *major groove* and the *minor groove*. These grooves arise because the glycosidic bonds of a base pair are not diametrically opposite each other (Figure 27.7).

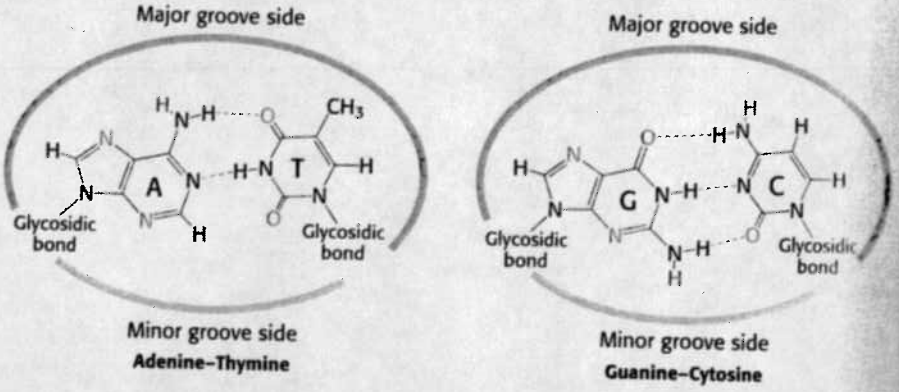

FIGURE 27.7 Major- and minor-groove sides. Because the two glycosidic bonds are not diametrically opposite each other, each base pair has a larger side that defines the major groove and a smaller side that defines the minor groove. The grooves are lined by potential hydrogen-bond donors (blue) and acceptors (red).

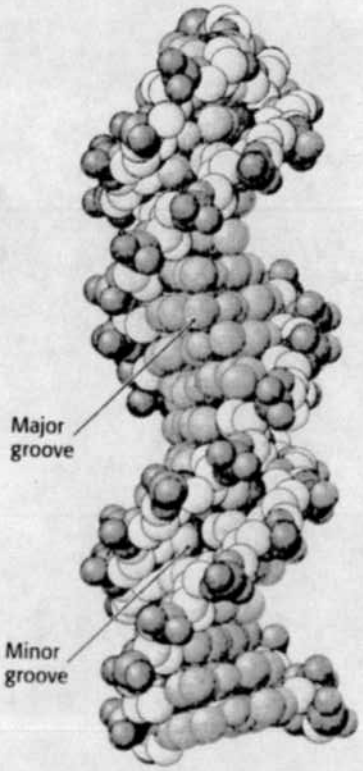

FIGURE 27.8 Major and minor grooves in B-form DNA. The major groove is depicted in orange, and the minor groove is depicted in yellow. The carbon atoms of the backbone are shown in white.

The minor groove contains the pyrimidine O-2 and the purine N-3 of the base pair, and the major groove is on the opposite side of the pair. The methyl group of thymine also lies in the major groove. In B-DNA, the major groove is wider (12 versus 6 Å) and deeper (8.5 versus 7.5 Å) than the minor groove (Figure 27.8).

Each groove is lined by potential hydrogen-bond donor and acceptor atoms that enable specific interactions with proteins (see Figure 27.7). In the minor groove, N-3 of adenine or guanine and O-2 of thymine or cytosine can serve as hydrogen acceptors, and the amino group attached to C-2 of guanine can be a hydrogen donor. In the major groove, N-7 of guanine or adenine is a potential acceptor, as are O-4 of thymine and O-6 of guanine. The amino groups attached to C-6 of adenine and C-4 of cytosine can serve as hydrogen donors. Note that the major groove displays more features that distinguish one base pair from another than does the minor groove. The larger size of the major groove in B-DNA makes it more accessible for interactions with proteins that recognize specific DNA sequences.

27.1.3 The Results of Studies of Single Crystals of DNA Revealed Local Variations in DNA Structure

X-ray analyses of single crystals of DNA oligomers had to await the development of techniques for synthesizing large amounts of DNA fragments

Introduction to Nucleic Acids:
Forces That Stabilize Nucleic Acid Double Helices

Before we begin describing the structural features of the oligonucleotides and double helices, a few remarks about the forces that govern base-base interactions are required. Two different interactions exist: a) those in the plane of the bases (horizontal); most commonly hydrogen bonds; b) those perpendicular to the base planes or "base stacking" effects; these are stabilized by London dispersion forces and the hydrophobic effect.

1) Hydrogen bonds.

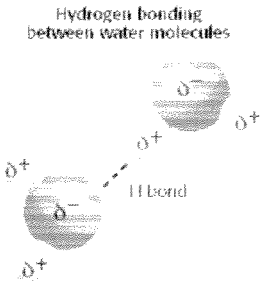

Hydrogen bonds are electrostatic in character. In general a hydrogen bond

X - H ··· Y

is formed if a hydrogen atom connects two atoms of higher electronegativity. Since these bonds are electrostatic, their strength depends on the partial charges located on the component atoms in the bond. The interaction between two water molecules, probably the most common hydrogen bonding interaction on the planet looks like this (Figure 14):

Figure 14

Under the influence of a hydrogen bond, the H becomes more electropositive and X,Y becoming more negative. This affect increases the affinity of X,Y for H and strengthens the interaction. If Y is the oxygen of the -OH group, the hydrogen attached to it is more positive and hence becomes a better donor.

Table 2 Comparison of Some Energy Values in Covalent and Hydrogen Bonds

Bond type	Bond length Å	Bond energy kcal/mole	Energy required for lengthening by 0.1 Å kcal/mole
Covalent			
C–C	1.54 ± 0.02	83.1	3.25
C–H (in ethane)	1.09 ± 0.02[a]	98.8[b]	3.60[c]
Hydrogen bond			
O–H · · · O	2.75 ± 0.2[d] (O · · · O distance)	3 to 6[e]	0.1[b]

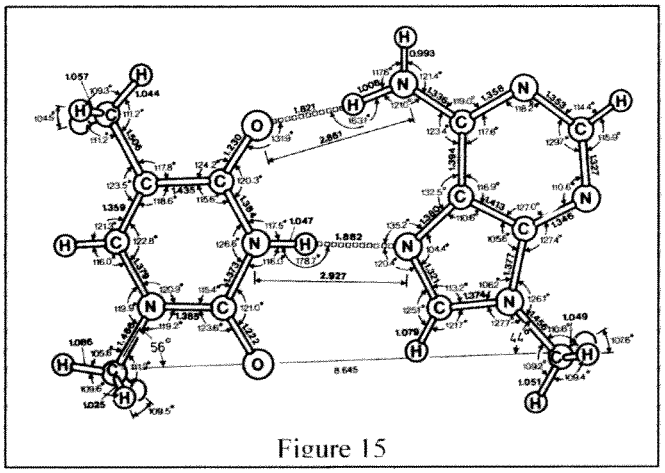

Figure 15

As you should already know, the strength of the an H bond is 20-30X weaker than a covalent bond. This weakness is reflected both in the bond's greater length and is relatively weak directionality **(TABLE 2)**.This weakness should not be mistaken for insignificance!!!! Moreover, the "slop" in directionality is not limitless. In fact, the tolerable distortion level in the angle of a hydrogen bond measured between the vector of the bond and the angle of the X - H bond is less than 20°. That is to say that the most favorable hydrogen bond angles are 180° **(FIGURE 15)**. Some bonds in the figure are distorted 27° and hence is weaker than the others distorted less than 2°.

2) Base Stacking.

Bases in solution pile up like coins in a roll. In aqueous solution, the bases in a single stranded oligonucleotide are stacked such that the base planes are separated by their van der Waals distance, 3.4 ?, parallel to one another. Base stacking is the least understood but, undoubtedly most important force stabilizing helices.

Stacking is a diffusion controlled, additive, and stabilized by weak forces. The enthalpies associated with base stacking are favorable, while the entropy associated with the stacking of the bases is strongly unfavorable. The stacking reaction is overall favorable, however, since the entropy and enthalpy of the solvent are both strongly favorable. Stacking is made-up of two separate forces: hydrophobic effect and London dispersion forces.

2a. Hydrophobic interactions.
If a hydrophobic base is dissolved in water, the water molecules cluster around it in an order fashion. This is caused by the fact that they cannot form H-bonds with the non-polar base and adopt an ordered "clathrate" structure to maximize H-bonding with itself. This ordering is a very unfavorable entropy change for the water. Burying this hydrophobic base in the stack, releases this water and results in an overall entropy gain for water (Figure 16).

A **B**

Figure 16

The importance of the hydrophobic effect in helix formation is seen by considering the effect on the energetics of solvent interactions upon folding the non-polar bases into the helical structure. Folding the polar backbone atoms, into a regular structure has slightly unfavorable ? H and slightly unfavorable TΔS. The effect of burying the non-polar side chains is dramatic, the T? S of the solvent is incredibly favorable, and the ΔH is also favorable (owing to the now completely satisfied H-bonding potential of the solvent).

2b. London Dispersion forces.
The bases stack upon one another at their van der Waals distance. It is at this distance where two molecules have an attraction for one another. This attraction, termed a van der Waals interactions is a gravitational forces. At too close a distance the electron of the two approaching molecules overlap, causing repulsion. At any given instant, the electronic charge distribution within atomic groups is asymmetric due to electron fluctuation, Therefore, dipoles created in on group of atoms polarize the electronic system of the the neighboring atoms or molecules, thus inducing parallel dipoles that attract each other.

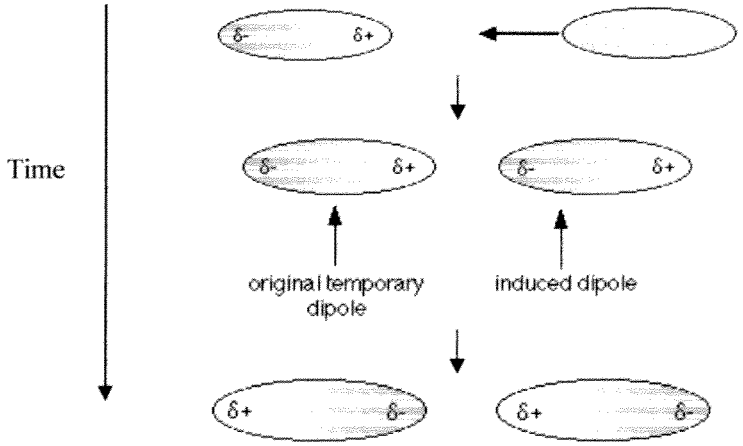

These forces are additive and are extremely distance dependent, falling off with the sixth power of distance (r^6).

There is no reason why this induced dipolar interaction has to be restricted to two molecules. As long as the molecules are close together this synchronized movement of the electrons can occur over huge numbers of molecules.

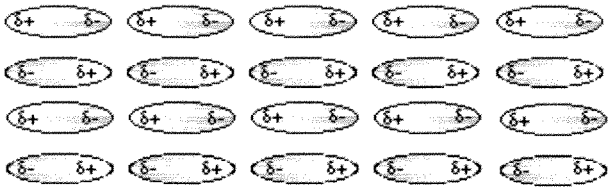

Since London dispersion attraction depends on formation of induced dipoles, the polarizable p electron cloud of the aromatic bases is extremely important. Therefore, stacking requires aromaticity of the bases-nonaromatic bases do not display stacking interactions. The strength of stacking interactions depends on how polarizable the p electron cloud of a base is. This in turn depends on the e- withdrawing or donating potential of the base substituents. These determine the primary basis for base stacking which is the electron structure of the bases. Since all bases have different substituents, the stacking potential of the bases are all different. Additionally, the electronic structure of a base can be modified by chemical modification-e.g., alkylation, halogenation.

Table 3 Total Stacking Energies [kcal/mole dimer] for the Ten Possible Dimers in B-DNA Type Arrangement Obtained by Quantum Chemical Calculations[a] [From (542)]

Stacked dimers	Stacking energies [kcal/mole dimer]
↑C·G / G·C↓	−14.59
↑C·G / A·T↓ ↑T·A / G·C↓	−10.51
↑C·G / T·A↓ ↑A·T / G·C↓	− 9.81
↑G·C / C·G↓	− 9.69
↑G·C / G·C↓ ↑C·G / C·G↓	− 8.26
↑T·A / A·T↓	− 6.57
↑G·C / T·A↓ ↑A·T / C·G↓	− 6.57
↑G·C / T·A↓ ↑T·A / C·G↓	− 6.78
↑A·T / A·T↓ ↑T·A / T·A↓	− 5.37
↑A·T / T·A↓	− 3.82

[a] Arrows designate direction of sugar phosphate chain and point from $C_{3'}$ of one sugar unit to $C_{5'}$ of the next, both carbons attached to the same phosphodiester link.

Stacking is BOTH base composition and base sequence dependent. In general, the stacking interactions of base paired nucleotide dimers containing G+C base pairs are more stable than those containing A+T base pairs **(TABLE 3)**.

Another generalization that can be made is that

3'pyrimidine purine5'
5'purine pyrimidine3'

is more stable than

3'purine pyrimidine5'
5'pyrimidine purine3'

For example $(5'G\text{-}C3')_2$ is 5kcal/mol more stable than $(5'C\text{-}G3')_2$. The origin of this sequence-energy correlation is seen in **FIGURE 17**. In the alternating purine,pyrimidine sequences, overlap between adjacent base pairs in a stack is much greater in B-DNA the pyrimidine, purine alternation, note the polar groups placed over the center of the p electron cloud, than the purine-purine stack.

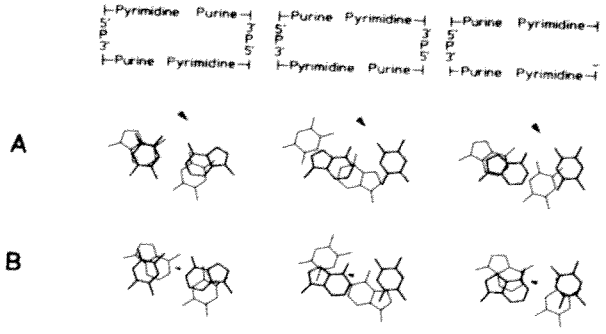

Figure 17 Base stacking overlaps in A- and B-type double helices, illustrated from top to bottom for A-, B-, and D-DNA. A–T base-pairs are stacked in sequences T–A on A–T, A–T on T–A, and A–T on A–T. The T–A on T–A stacking is comparable to A–T on A–T, with top and bottom reversed. Because views are perpendicular to base-pairs and not along the helix axes, the latter project as lines, indicated by arrows pointing from upper to lower base-pair. Note that in A- and D-DNA, arrows point in opposite directions because in the former the tilt positive and negative in the latter. The arrow in B-DNA is smallest because the tilt is only slightly negative. For C-DNA the stacking patterns are between B- and D-DNA. Redrawn from (845).

Helical Formation

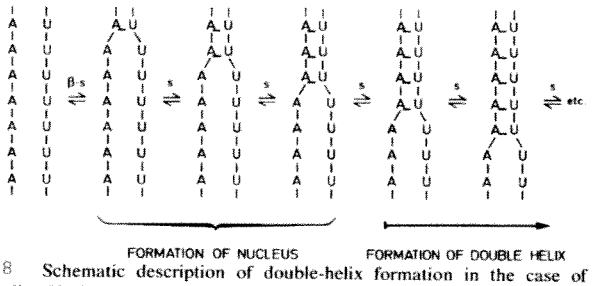

Figure 18 Schematic description of double-helix formation in the case of oligo(A)·oligo(U). In this system, helix growth parameter s is about 10 at 0°C and 1 at the melting temperature. Nucleation parameter β, 10^{-3} liters/mole, diminishes stability constant $K = \beta \cdot s$ of primary base-pair formation but does not influence formation of additional, stacked base-pairs which form cooperatively with $K = s$ according to a *linear Ising model*. In constrast to the *isodesmic model* for base stacking (Figure 6-9), where each step is independent of the other, in the *cooperative process* described by the Ising model, base-pair formation and stacking are influenced by the next neighbors, except for the very first base–base association.

Let us now turn to how both base stacking and H-bond formation are involved in helix formation. The association of double stranded polynucleotide helices is a cooperative process. One can think of helix formation as analogous to closing a zipper. The first step is association of the a single base pair with a stability constant expressed as the product of a nucleation parameter, b, which essentially represents the unfavorable entropy of bringing together two ends of separate chains and a chain growth parameter, *s*, which represents the favorable aspects of hydrogen bonding and hydrophobic interactions **(FIGURE 18)**.

The addition of a second stacked base pair is not influenced by the nucleation parameter because the proximity effect is taken care of in the first association. This is the basis of the cooperativity of helix formation, **base pair formation and stacking are influenced by the nearest neighbors, except for the first base pair formed**. Because of the overall unfavorability of the nucleation constant, ß, the energy of helix formation is unfavorable until after about three base pairs have formed. From then on, growth of the double helix is spontaneous, due mainly to the geometrical constraints of the sugar phosphate backbone, as implied by the sterochemistry of the nucleotide unit, whose preferred configurations is preset to form a double helix. Also, the summation of these weak forces, over a number of nucleotides provide cooperative energy. This is illustrated schematically in **FIGURE 19** and quantitatively expressed by K, the helical stability constant.

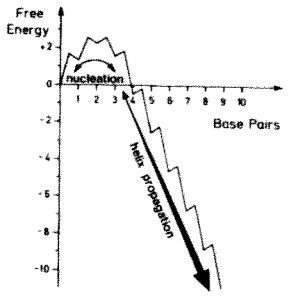

Figure 19 After the unfavorable positive free energy contribution in the nucleation process is overcome, the free energy for additional steps becomes negative and the helix grows spontaneously. Relative total free energy (ΔG) of helix formation in arbitrary units is plotted as a function of the number of consecutive, stacked base-pairs assembled into a helical array. From (544).

$$K = (\beta * s) * (n * s)$$

where ß<1 ($\sim 10^{-3}$ *l* M^{-1}), s= 10 @ 0°C and 1 @ T_m and n=number of base pairs

Helical Breakdown/Denaturation (Melting)

The denaturation of a double helix is also cooperative, for much the same reasons as the formation is. In unzipping a helix, a bulge is formed due to input of energy. These bases are unable to H-bond with solvent and the solvent is order around the aromatic ring. In order to relieve this unfavorable situation, a nucleus of stacked single-stranded polynucleotide is formed which has favorable van der Waals interactions and has reduced hydrophobic surface in contact with the solvent. Then on the same ideas for unzipping apply as for zipping

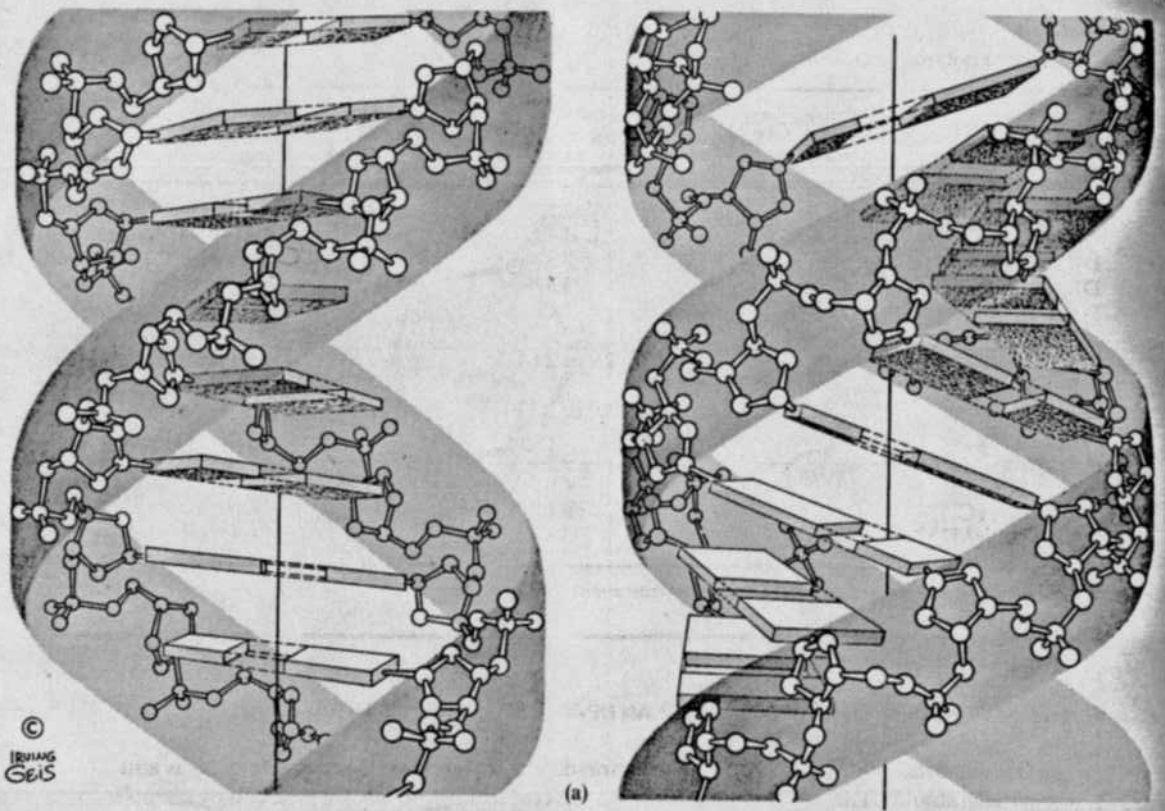

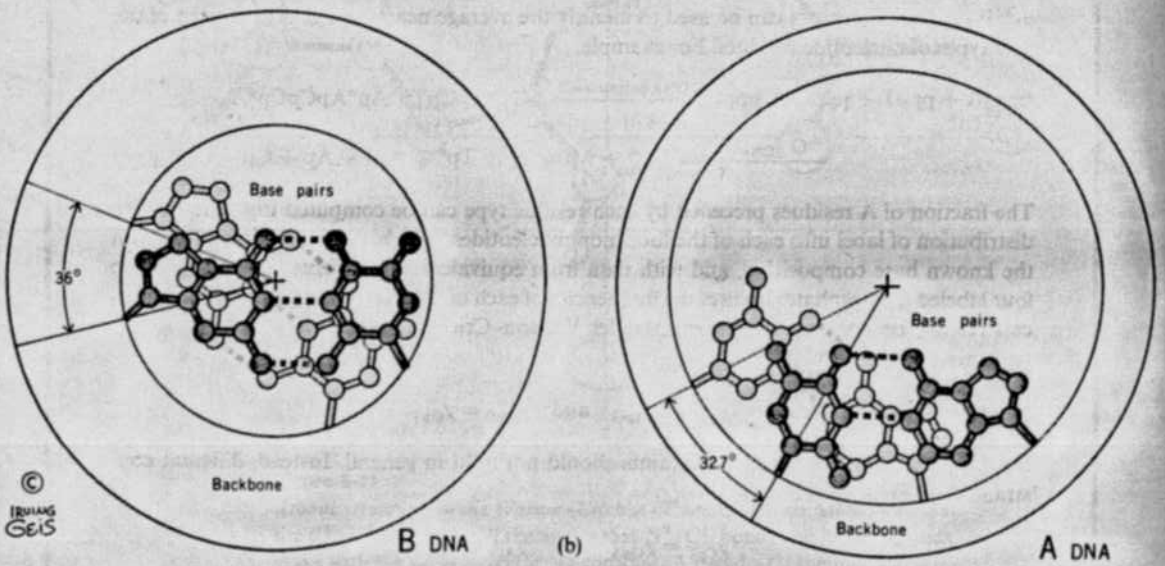

2.1

Figure 3-12

The DNA-B and DN
illustrations each ba
explicitly drawn. Th
axis (+). In DNA B
rotate around the ir
After computer dra

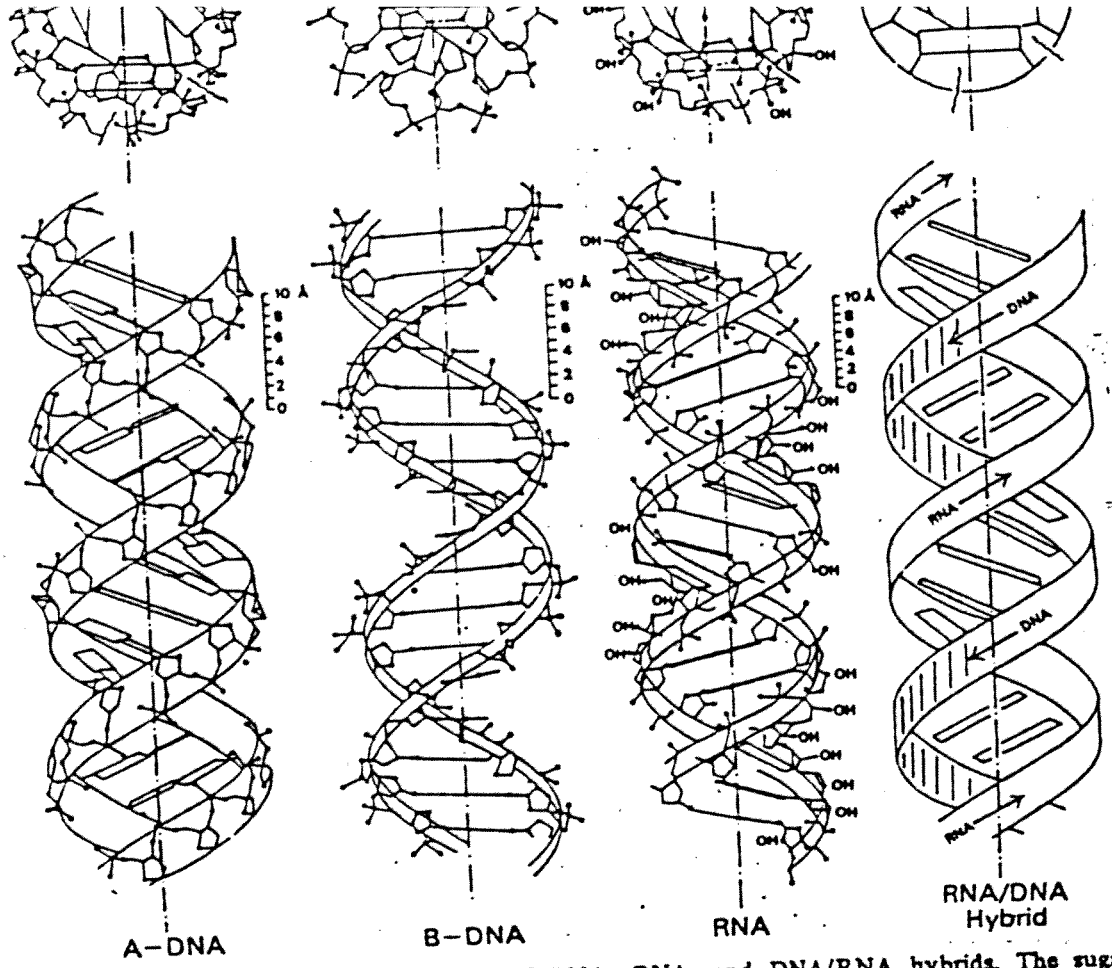

FIG 1.6 Double helical structures of DNA, RNA, and DNA/RNA hybrids. The sugar-phosphate backbone is represented thus ⌒⌒..., and base pairs as ▭. Re-drawn from Yang and Sameiima (1969).

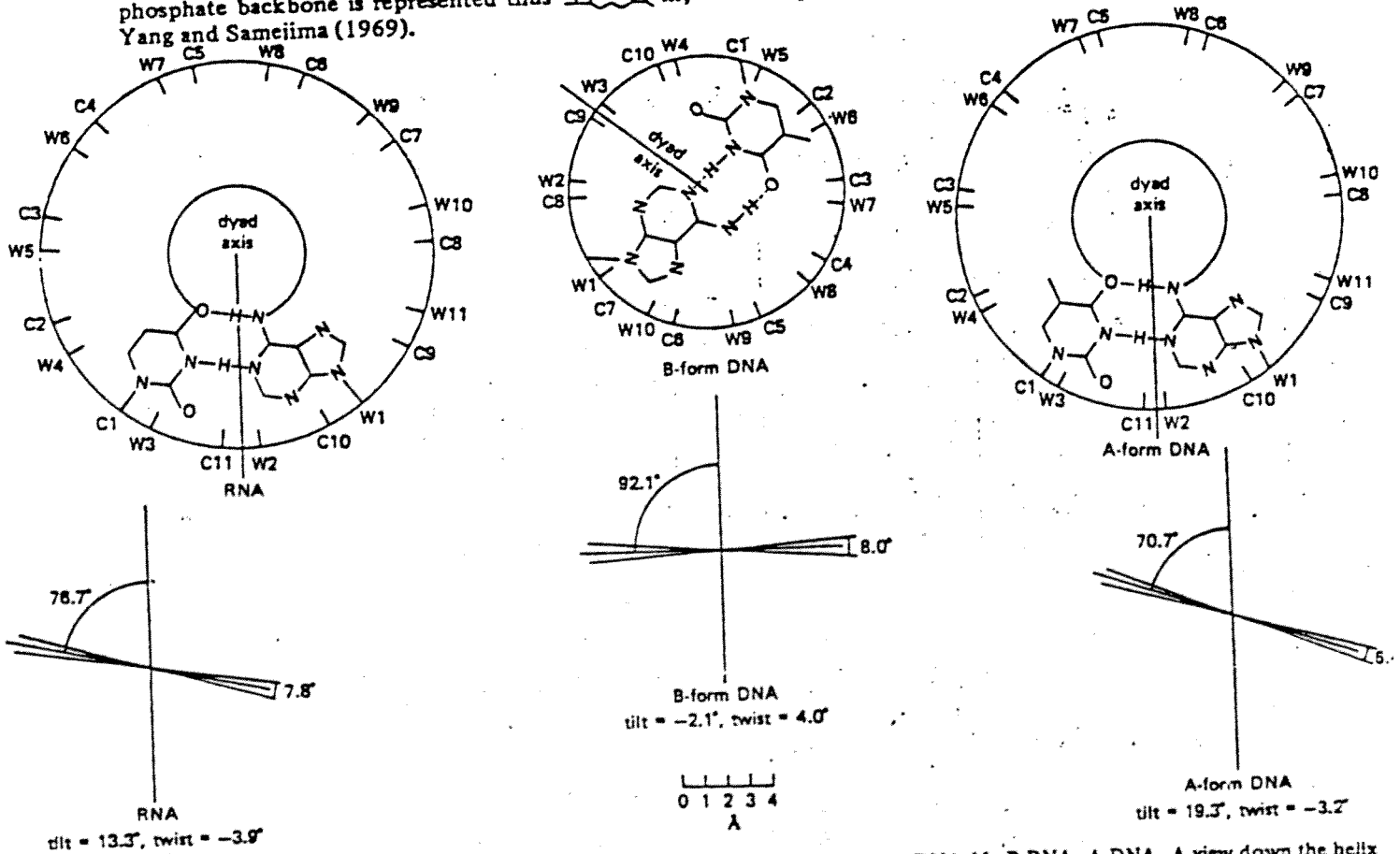

FIGURE 4-11 The geometry of Watson-Crick base pairs in three double-stranded structures: RNA 11, B-DNA, A-DNA. A view down the helix axis is given on the left. The dyad axis is the two-fold symmetry axis for the strands. Rotation of 180° about this axis leaves all sugar and phosphate atoms unchanged. Positions of successive base pairs in one turn of the helix are labeled C2:W2, etc. The angle that the average plane of the base pairs makes with the helix axis (tilt) and the dihedral angle between bases (twist) is shown on the right. [Data from S. Arnott, S. D.

5.1

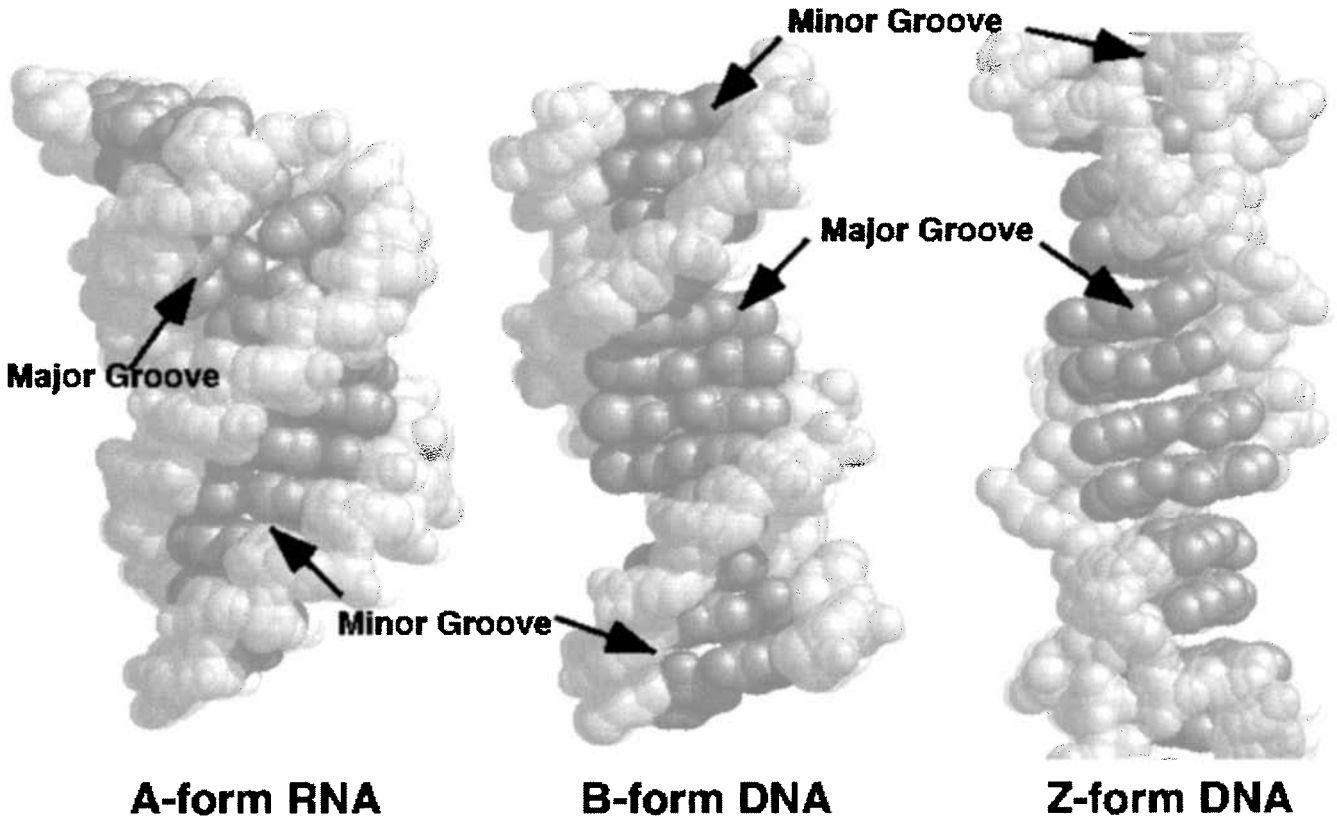
Minor Groove
Major Groove
Major Groove
Minor Groove
A-form RNA
B-form DNA
Z-form DNA

2.3

disappears.[6]

Predicting Z-DNA structure

It is possible to predict the likelihood of a DNA sequence forming a Z-DNA structure. An algorithm for predicting the propensity of DNA to flip from the B-form to the Z-form, *ZHunt*, was written by Dr. P. Shing Ho in 1984 (at MIT).[7] This algorithm was later developed by Tracy Camp, P. Christoph Champ, Sandor Maurice, and Jeffrey M. Vargason for genome-wide mapping of Z-DNA (with P. Shing Ho as the principal investigator).[8]

Z-Hunt is available at Z-Hunt online.

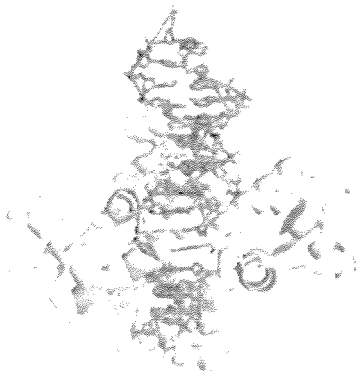

B-/Z-DNA junction bound to a Z-DNA binding domain. Note the two highlighted extruded bases. From PDB 2ACJ.

Biological significance

While no definitive biological significance of Z-DNA has been found, it is commonly believed to provide torsional strain relief (supercoiling) while DNA transcription occurs.[9][2] The potential to form a Z-DNA structure also correlates with regions of active transcription. A comparison of regions with a high sequence-dependent, predicted propensity to form Z-DNA in human chromosome 22 with a selected set of known gene transcription sites suggests there is a correlation.[8]

Z-DNA formed after transcription initiation in some cases may be bound by RNA modifying enzymes, such as ADAR1[*citation needed*], which then alter the sequence of the newly-formed RNA.[10]

In 2003, Biophysicist Alexander Rich of the Massachusetts Institute of Technology noticed that a poxvirus virulence factor, called E3L, mimicked a mammalian protein that binds Z-DNA.[11][12] In 2005, Rich and his colleagues pinned down what E3L does for the poxvirus. When expressed in human cells, E3L increases by five- to 10-fold the production of several genes that block a cell's ability to self-destruct in response to infection.

Rich speculates that the Z-DNA is necessary for transcription and that E3L stabilizes the Z-DNA, thus prolonging expression of the anti-apoptotic genes. He suggests that a small molecule that interferes with the E3L binding to Z-DNA could thwart the activation of these genes and help protect people from pox infections.

Comparison Geometries of Some DNA Forms

Geometry attribute	A-form	B-form	Z-form
Helix sense	right-handed	right-handed	left-handed
Repeating unit	1 bp	1 bp	2 bp
Rotation/bp	32.7°	35.9°	60°/2
bp/turn	11	10.5	12
Inclination of bp to	+19°	−1.2°	−9°

Side view of A-, B-, and Z-DNA.

2.4

axis			
Rise/bp along axis	2.3 Å (0.23 nm)	3.32 Å (0.332 nm)	3.8 Å (0.38 nm)
Pitch/turn of helix	28.2 Å (2.82 nm)	33.2 Å (3.32 nm)	45.6 Å (4.56 nm)
Mean propeller twist	+18°	+16°	0°
Glycosyl angle	anti	anti	C: anti, G: syn
Sugar pucker	C3'-endo	C2'-endo	C: C2'-endo, G: C2'-exo
Diameter	23 Å (2.3 nm)	20 Å (2.0 nm)	18 Å (1.8 nm)

Sources: [13][14][15]

See also

- Mechanical properties of DNA
- DNA supercoil
- DNA
- A-DNA
- B-DNA
- Z-DNA binding protein 1 (ZBP1)
- Zuotin
- E3L
- ADAR1
- *Proteopedia Z-DNA*

References

1. ^ Wang AHJ, Quigley GJ, Kolpak FJ, Crawford JL, van Boom JH, Van der Marel G, Rich A (1979). "Molecular structure of a left-handed double helical DNA fragment at atomic resolution". *Nature (London)* **282** (5740): 680–686. doi:10.1038/282680a0. PMID 514347.
2. ^ *a b* Ha SC, Lowenhaupt K, Rich A, Kim YG, Kim KK (2005). "Crystal structure of a junction between B-DNA and Z-DNA reveals two extruded bases". *Nature* **437** (7062): 1183–1186. doi:10.1038/nature04088. PMID 16237447.
3. ^ Placido D, Brown BA 2nd, Lowenhaupt K, Rich A, Athanasiadis A (2007). "A left-handed RNA double helix bound by the Zalpha domain of the RNA-editing enzyme ADAR1". *Structure* **15** (4): 395–404. doi:10.1016/j.str.2007.03.001. PMC 2082211. PMID 17437712. http://www.pubmedcentral.nih.gov/articlerender.fcgi?tool=pmcentrez&artid=2082211.
4. ^ Hall K, Cruz P, Tinoco I Jr, Jovin TM, van de Sande JH (October 1984). "'Z-RNA'--a left-handed RNA double helix". *Nature* **311** (5986): 584–586. doi:10.1038/311584a0. PMID 6482970.
5. ^ de Rosa M, de Sanctis D, Rosario AL, Archer M, Rich A, Athanasiadis A, Carrondo MA (2010-05-18). "Crystal structure of a junction between two Z-DNA helices". *Proc Natl Acad Sci USA* **107** (20): 9088–9092. doi:10.1073/pnas.1003182107. PMC 2889044. PMID 20439751. http://www.pubmedcentral.nih.gov/articlerender.fcgi?tool=pmcentrez&artid=2889044.
6. ^ Zhang H, Yu H, Ren J, Qu X (2006). "Reversible B/Z-DNA transition under the low salt condition and non-

Two polynucleotide chains running in opposite directions coil around a common axis to form a right-handed double helix.

Purine and pyrimidine bases are on the inside of the helix, whereas phosphate and deoxyribose units are on the outside.

Adenine (A) is paired with thymine (T), and guanine (G) with cytosine (C). An A–T base pair is held together by two hydrogen bonds, and that of a G–C base pair by three such bonds.

27.1.1 A-DNA Is a Double Helix with Different Characteristics from Those of the More Common B-DNA

Watson and Crick based their model (known as the *B-DNA helix*) on x-ray diffraction patterns of DNA fibers, which provided information about properties of the double helix that are averaged over its constituent residues. The results of x-ray diffraction studies of dehydrated DNA fibers revealed a different form called *A-DNA*, which appears when the relative humidity is reduced to less than about 75%. A-DNA, like B-DNA, is a right-handed double helix made up of antiparallel strands held together by Watson-Crick base pairing. The A helix is wider and shorter than the B helix, and its base pairs are tilted rather than perpendicular to the helix axis (Figure 27.4).

Many of the structural differences between B-DNA and A-DNA arise from different puckerings of their ribose units (Figure 27.5). In A-DNA, C-3′ lies out of the plane (a conformation referred to as C-3′-endo) formed by the other four atoms of the furanose ring; in B-DNA, C-2′ lies out of the

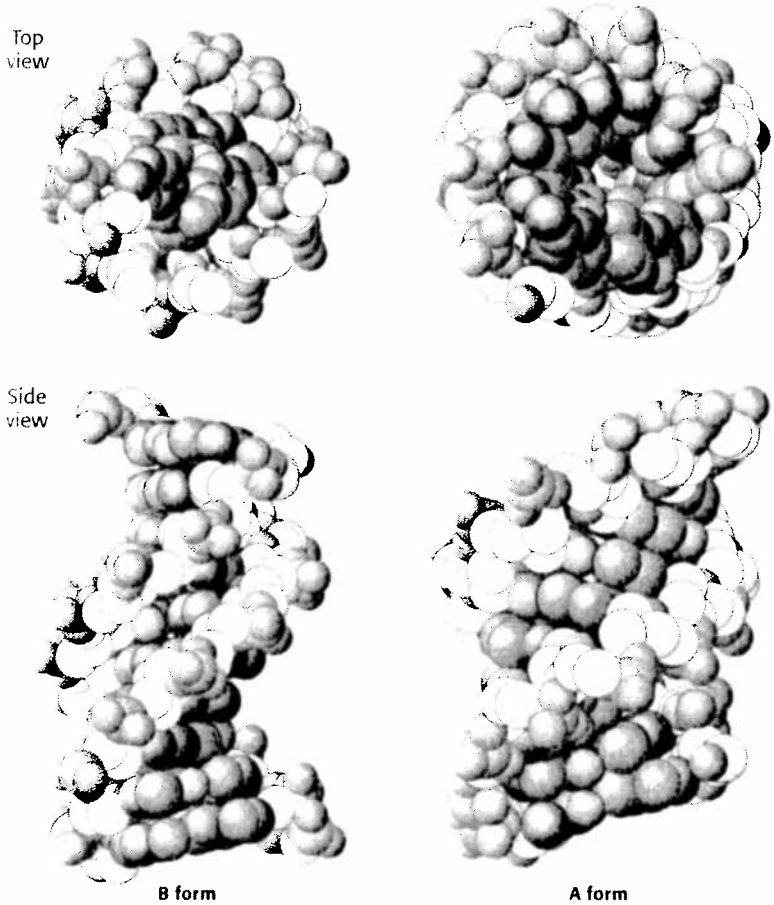

FIGURE 27.4 B-form and A-form DNA. Space filling models of ten base pairs of B form and A form DNA depict their right handed helical structures. The B form helix is longer and narrower than the A form helix. The carbon atoms of the backbone are shown in white.

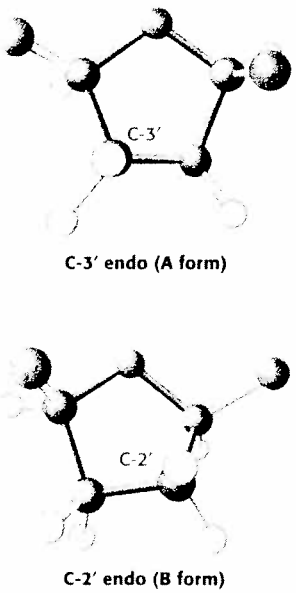

FIGURE 27.5 Sugar puckers. In A form DNA, the C-3′ carbon atom lies above the approximate plane defined by the four other sugar nonhydrogen atoms (called C-3′ endo). In B-form DNA, each ribose is in a C-2′ endo conformation.

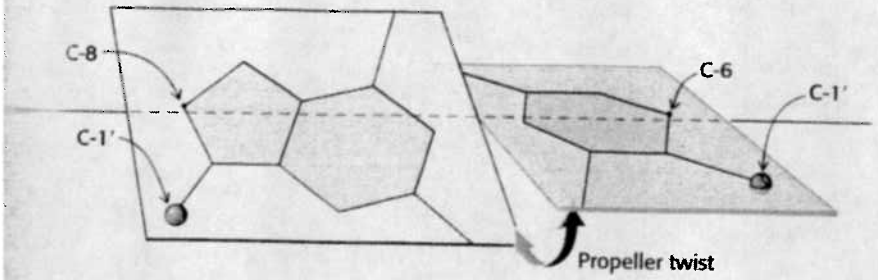

FIGURE 27.9 Propeller twist. The bases of a DNA base pair are often not precisely coplanar. They are twisted with respect to each other, like the blades of a propeller.

ith defined base sequences. X-ray analyses of single crystals of DNA at tomic resolution revealed that *DNA exhibits much more structural variabil-y and diversity than formerly envisaged.*

The x-ray analysis of a crystallized DNA dodecamer by Richard Dick-rson and his coworkers revealed that its overall structure is very much like B-form Watson-Crick double helix. However, the dodecamer differs from he Watson-Crick model in not being uniform; there are rather large local eviations from the average structure. The Watson-Crick model has 10 esidues per complete turn, and so a residue is related to the next along a hain by a rotation of 36 degrees. In Dickerson's dodecamer, the rotation ngles range from 28 degrees (less tightly wound) to 42 degrees (more tightly ound). Furthermore, the two bases of many base pairs are not perfectly planar (Figure 27.9). Rather, they are arranged like the blades of a pro-eller. This deviation from the idealized structure, called *propeller twisting,* hances the stacking of bases along a strand. These and other local varia-ons of the double helix depend on base sequence. A protein searching for specific target sequence in DNA may sense its presence through its effect the precise shape of the double helix.

7.1.4 Z-DNA Is a Left-Handed Double Helix in Which ackbone Phosphates Zigzag

lexander Rich and his associates discovered a third type of DNA helix hen they solved the structure of dCGCGCG. They found that this hexa-cleotide forms a duplex of antiparallel strands held together by Watson-ick base-pairing, as expected. What was surprising, however, was that s double helix was *left-handed,* in contrast with the *right-handed* screw se of the A and B helices. Furthermore, the phosphates in the backbone *zagged;* hence, they called this new form *Z-DNA* (Figure 27.10).

The Z-DNA form is adopted by short oligonucleotides that have *uences of alternating pyrimidines and purines.* High salt concentrations required to minimize electrostatic repulsion between the backbone

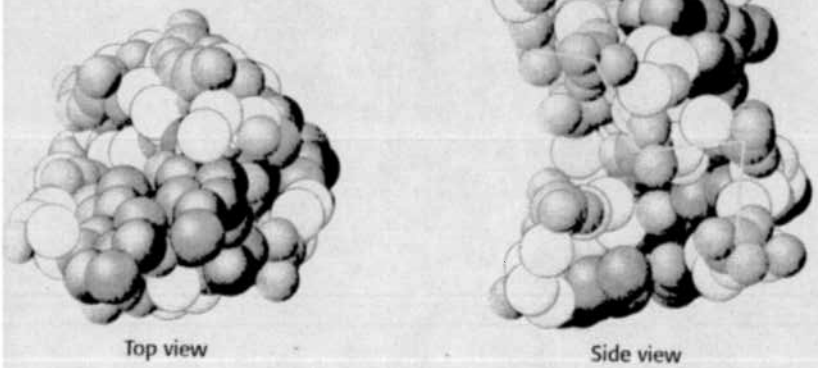

FIGURE 27.10 Z-DNA. DNA oligomers such as dCGCGCG adopt an alternative conformation under some conditions. This conformation is called Z-DNA because the phosphate groups zigzag along the backbone.

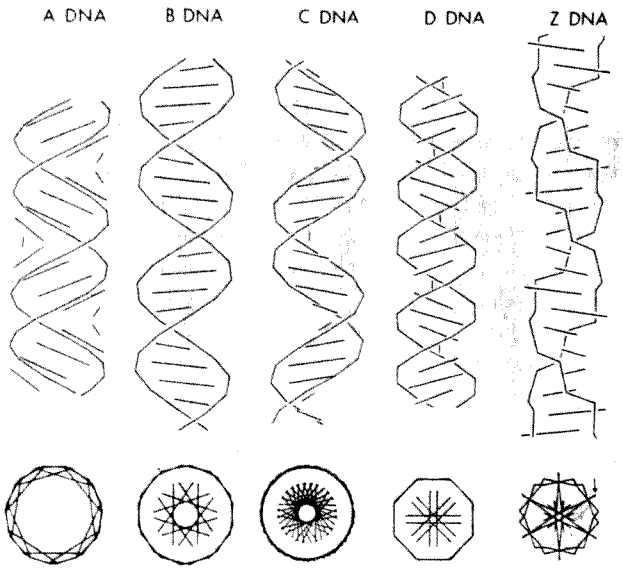

Figure 1 Models for various conformations of DNA. Segments containing 20 base pairs are shown for right-handed models of A (31), B (31), C (32) or D DNA (33) and for the left-handed Z_I form of DNA (34). The upper views are perpendicular to the helical axes and the lower views look along the helical axes. The continuous helical lines are formed by linking the phosphorus atoms along each strand. The line segments indicate the positions of the base pairs and are formed by joining the C1' atoms of each base pair. This simplified mode of representation emphasizes the differences in helical parameters and in positions of the base pairs among these models. The arrow in the lower view of Z DNA indicates the C1' of the deoxyguanosine residue, the base of which is relatively exposed in this structure (see text); the deoxycytidine residue is more centrally located.

(1972)

diffraction pattern. Arnott & Hukins (31) refined this structure and provided a set of atomic coordinates that have been widely used in discussions of B DNA. Certain aspects of the B form are not presently controversial: all current models assume a double helix with antiparallel strands and with Watson-Crick base pairs oriented roughly at right angles to the helix axis (Figure 1). Controversy exists as to whether the helix is right-or left-handed or both, as to the exact number of base pairs/turn, and as to the disposition of the bases (coplanarity of bases within the pairs and their orientation with respect to the helix axis).

Most DNA can adopt the B form as defined by its characteristic X-ray fiber diffraction pattern: The bulk of the sequences of natural DNA over a wide range of base compositions (51, 52) as well as synthetic DNA of several simple base sequences (35) yields the B pattern under appropriate

DNA conformation	Occurrence	Axial rise per base pair (Å)	Base pairs per turn	Base pairs per repeating unit	Ref
A	Most natural and synthetic DNA	2.6	11.0	1	31, 35, 36
B	Most natural and synthetic DNA	3.4	10.0[a]	1	31, 35, 37
Alternating B	Several alternating purine-pyrimidine DNA	3.4	10.0	2	38
C	Most natural and synthetic DNA	3.3	7.9–9.6	1	33, 35, 39, 40
D	Several synthetic DNA	3.0	8.0	1	33, 35, 41
T	Glucosylated bacteriophage DNA	3.3–3.4	8.0–8.4	1	42, 43
Z	Several alternating purine-pyrimidine DNA	3.6–3.8	12.0	2	34, 44–46

[a] Alternative models with different parameters are discussed in text.

conditions. Further, the patterns are similar to each other in detail, which suggests a narrow range of variability in B form structure. This apparent homogeneity is in contrast to recent suggestions from nondiffraction techniques and from single-crystal diffraction studies on oligonucleotides, which indicate either static or dynamic structural heterogeneity (see below). Early indications of deviant structures in DNA of high AT-content have been correlated with the presence of non-DNA material (53). There are a few species of synthetic DNA, namely poly(dA)·poly(dT), poly(dI)·poly(dC), and poly(dA-dI)·poly(dC-dT), that have a B form that is significantly different from that of the other complementary deoxypolymers. These polymers have different intermolecular packing arrangements and a slightly changed value for the rise per residue (35, 54). A striking indication of altered structure or structures for the conformations of poly(dA)·poly(dT) and poly(dI)·poly(dC) is their refusal to undergo a transition from the B form to the A form (35, 54–56). These unusual properties assume particular interest given the existence of relatively long dA·dT sequences in vivo (57).

B form adopted by self-complementary oligodeoxynucleotides The structure of a long self-complementary oligodeoxynucleotide, d(CGCGAATTCGCG), has recently been solved by single-crystal diffraction techniques (58–61). The dodecanucleotide forms more than a full turn of a helix whose

10

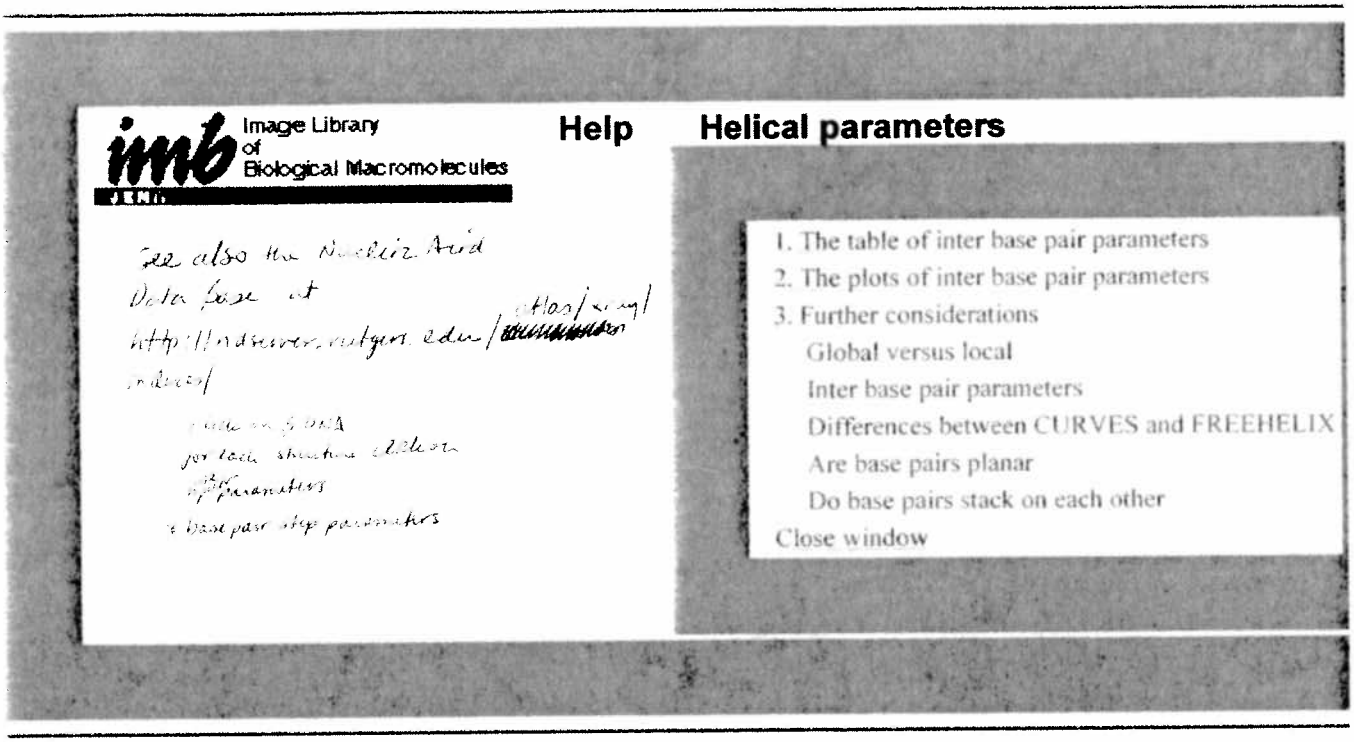

Helix and bending analysis of nucleic acid double helix structures

Helical parameters

1. The table of inter base pair parameters

The architecture of a nucleic acid double helices can be described in terms of helical parameters, which have been defined in the Cambridge convention (Dickerson, 1989). The helical parameters are derived from the spatial location of the bases, while the sugar phosphate backbone is not taken into account. The six inter base pairs parameters (*rise*, *twist*, *shift*, *roll*, *tilt*, *slide*) describe the local conformation of a double helix at every base pair step. A table of the inter base pair parameters calculated with respect to the curvilinear helical axis is presented on the '**Analysis of nucleic acid double helix geometry**' page. These parameters are calculated with CURVES.

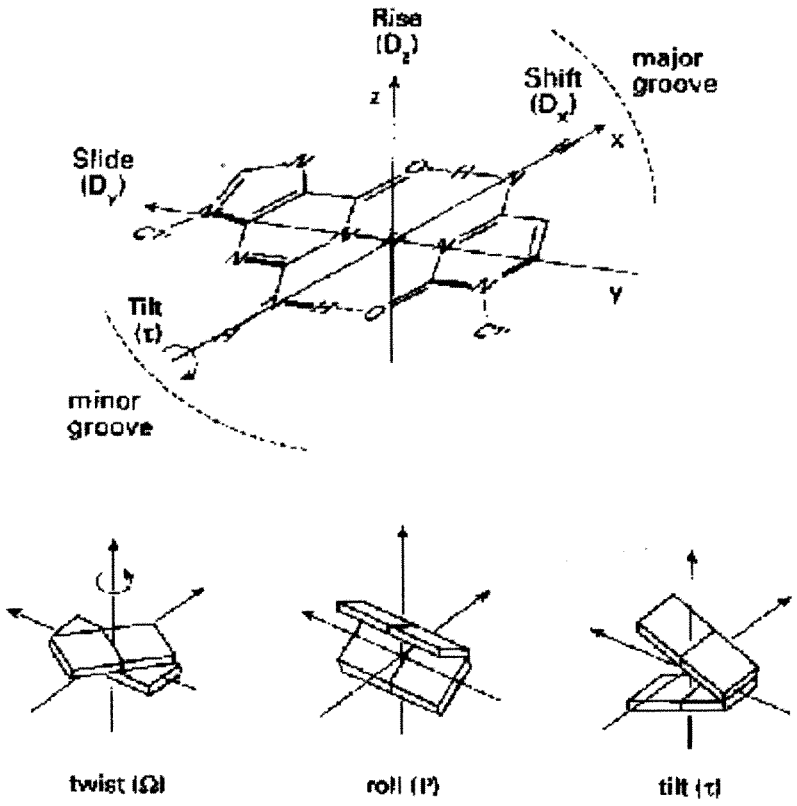

Figure 1. The six inter base pair parameters. (Blackburn GM, Gait MJ. 1996. Nucleic acids in chemistry and biology. Oxford University Press.)

2. The plot of inter base pair parameters

You can also request a plot of the six inter base pair parameters. These plots show three sets of the inter base pair parameters calculated with different approaches:

- CURVES inter base pair parameters calculated with respect to the global helical axis (black lines). These data are also given in the table of inter base pair parameters.
- CURVES inter base pair parameters calculated with respect to the local axes of each dinucleotide step and averaged for the two strands (red lines).
- FREEHELIX vector inter base pair parameters calculated with respect to the local axes of each base pair step (red lines).

Furthermore, also the *dinucleotide irregularity function* (DIF) from CURVES and the *angle between base pair normal vectors* from FREEHELIX are shown in the plot. Both graphs are useful to reveal at which base pair step the helix geometry is distorted.

Local distortions of the helix geometry do not necessarily result in a global bending of the helix. A helix is straight, if the helical parameters are regular, but also if all local distortions cancel each other. Bending occurs, if there is either a single local distortion or if various local distortions add up to a global effect. It is intended that users compare the table and the plot of the helical parameters with the images

12

and the geometrical parameters of the helical axis obtained from the '**Bending of the helical axis**' page. To facilitate such comparisons the 5'-end of strand 1 is always located at the left hand side, as well in the plots of helical parameters as in the front views of a helix or a helical axis. Accordingly, the 3'-end of strand 1 is always found at the right hand side. This is also the usual way of writing the sequence of a nucleic acid.

The helical parameters are vector quantities characterized by magnitude and direction. They point into different directions at each base pair step. The graphs show only the magnitude of these vectors. If you want to reveal the effect of a distortion of a single helical parameter on the global shape of the helix, you have to take into account also the magnitudes and the directions of all other helical parameters.

3. Further considerations

Global versus local

The terms global and local are used with two different meanings in the field of nucleic acid structure analysis. A global property of a molecular structure depends on all the atoms in the structure, while a local property arises if only a subset of neighboring atoms is used to determine that quantity. In this sense Lavery and Sklenar (1988) have defined global and local helical parameters, which both can be calculated with their program CURVES.

The global as well as the local inter base pair parameters are related to particular base pair steps. These parameters are vector quantities which have a defined location in 3-dimensional space and with respect to the nucleic acid sequence. In contrast, the average inter base pair parameters are scalar values which are not related to any part of the structure. They characterize properties of the whole structure. Confusingly now, the terms local and global are also used to indicate the scope of a property. Local parameters are related to parts of a structure while global parameters are valid for the whole structure. In this sense the global helical parameters from CURVES are also local.

Inter base pair parameters

In Figure 1 the base pairs are shown as planar plates. In a regular helix such planar elements are stacked on each other. Each step from one plate to the next can be described as a combination of a translational and a rotational movement. The translational and the rotational displacements are 3-dimensional vectors, which can be split into three orthogonal components. The three translational components are *rise*, *shift* and *slide*. *Rise* is a translation in the direction of the helical axis (**z**-axis), and *shift* is orthogonal to the helical axis and directs to the major groove side.

Twist, *roll* and *tilt* are the three rotational components. *Twist* is a rotation about the helical axis (**z**-axis). A positive *roll* indicates that there is a cleft between two stacked base pairs which opens towards the minor groove. A negative *roll* is related to an opening towards the major groove. The definitions of the six inter base pair parameters are rigorous but the Cambridge convention does not define how to establish the reference coordinate system. The decomposition of the total translational and rotational movement into orthogonal components depends crucially on the reference system used. Several different algorithms and programs exist for calculating the helical parameters. The algorithms differ mainly in the methods used to derive the reference coordinate systems.

Differences between CURVES and FREEHELIX

13

In general, most programs in the field yield similar results for regular B-DNA, but the differences are more pronounced for irregular helical stretches. Irregular helices are especially interesting because they occur in several DNA/protein complexes and also in unusual DNA structures like Holliday junctions and other intermediates of DNA recombination. The interpretation of such structures crucially depends on the method used to determine the helical parameters.

One of the merits of the CURVES approach is that it establishes a global helical axis for the whole structure. An optimization procedure is used to determine the best curvilinear axis. The coordinates of the atoms of all bases are employed simultaneously to determine this axis. In this sense CURVES calculates global helical parameters for every base pair step. Other approaches like FREEHELIX determine local helical parameters, where only the coordinates of the two base pairs involved are taken into account. When comparing helical parameters obtained from different methods we must always keep in mind that these parameters are vector quantities. The vectors will differ not only in their lengths but also in their directions.

CURVES can also determine local helical parameters. But these local parameters are different from the local parameters of FREEHELIX. FREEHELIX first fits planes to every base pair and then calculates the helical parameters between the planes. In this way averaging between the two strands is done first. CURVES calculates helical parameters separately for each strand and then does a pairwise averaging of all the parameters resulted for each strand.

If you want to compare two structures you should use helical parameters which have been determined with the same method. Helical parameters found in the literature have often been calculated with different programs or with different program options. Our helix analysis allows to obtain helical parameters calculated with a standardized method for all nucleic acid double helix structures deposited in the PDB and NDB.

Are base pairs planar?

The base pairs in nucleic acid structures are not really planar. For example, the propeller twist of AT base pairs in B-DNA is usually in the range of -15° to -20°. If the base pairs are not planar, the six inter base pair parameters will give only a rough model of the helix. A more detailed picture is obtained if also the intra base pair parameters are taken into account.

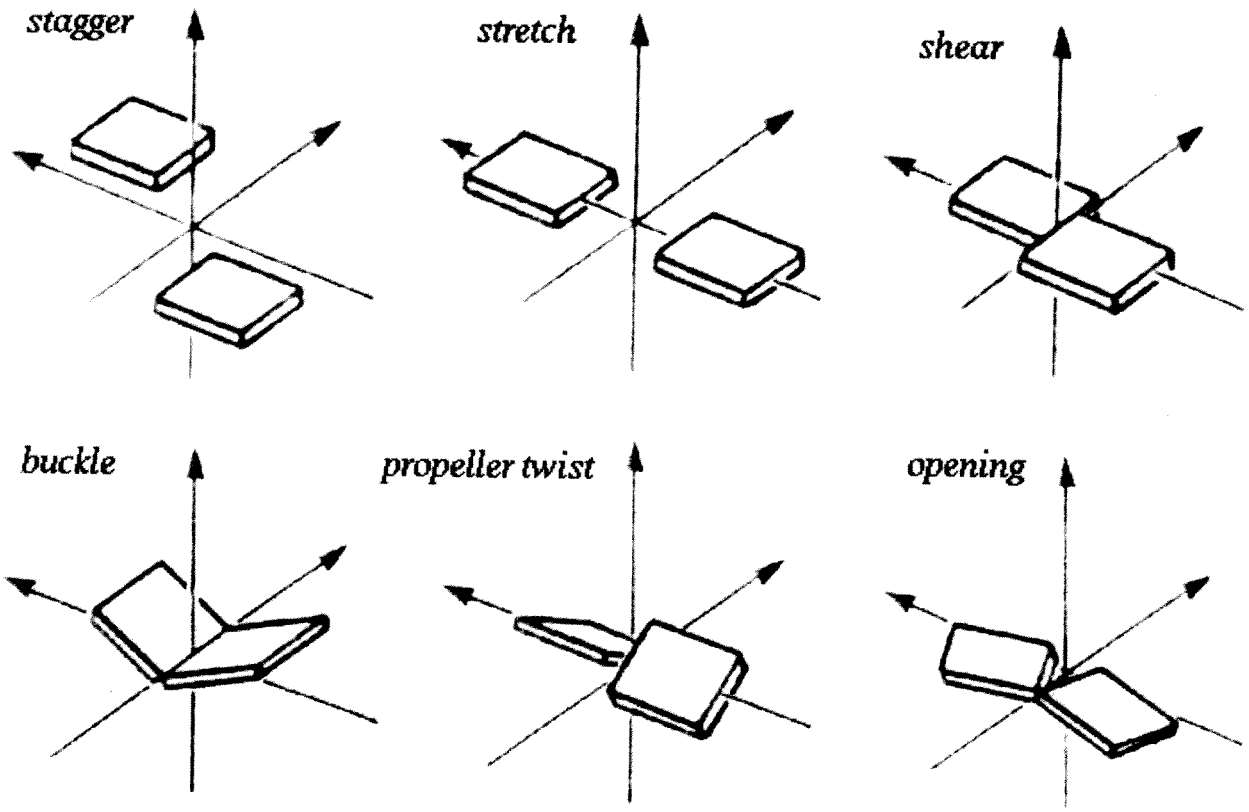

Figure 2. The three translational and three rotational displacements within a base pair. (Blackburn GM, Gait MJ. 1996. Nucleic acids in chemistry and biology. Oxford University Press.)

The Cambridge convention defines six base pair parameters which describe the deviation from planarity within a base pair (Figure 2). These six parameters describe the translational and rotational displacement between the two bases of a base pair. Again, the translational and rotational displacement is divided into orthogonal components. The translational components are *stagger*, *stretch* and *shear*, and the rotational components are *propeller twist*, *buckle*, *opening*. Instead of determining the (intra) base pair parameters, it is also possible to calculate the inter base pair separately for each strand. Both approaches yield twelve parameters for each base pair.

Do base pairs stack on each other?

The FREEHELIX approach (Dickerson, 1998) is based on the assumption that base pairs are the building blocks of a helix. The base pairs stack on each other to form a helix. Deviations from parallel stacking can be easily detected from the *angle between base pair normal vectors*. Dickerson has shown for some DNA/protein complexes that local unstacking of base pairs is related to global bending of the helix.

However, if the base pairs deviate significantly from planarity the FREEHELIX method of fitting a common plane to both bases becomes questionable. For non-planar base pairs it seems to be more important how the bases in each strand are stacked on each other. CURVES allows to calculate the inter base pair parameters separately for each strand. If you are interested in these parameters you can request the full output from CURVES and also from FREEHELIX on the '**Analysis of nucleic acid double helix geometry**' page. The output files also show precisely which program options are used.

Biol 515=1
1.19.89
notes - (V)
15

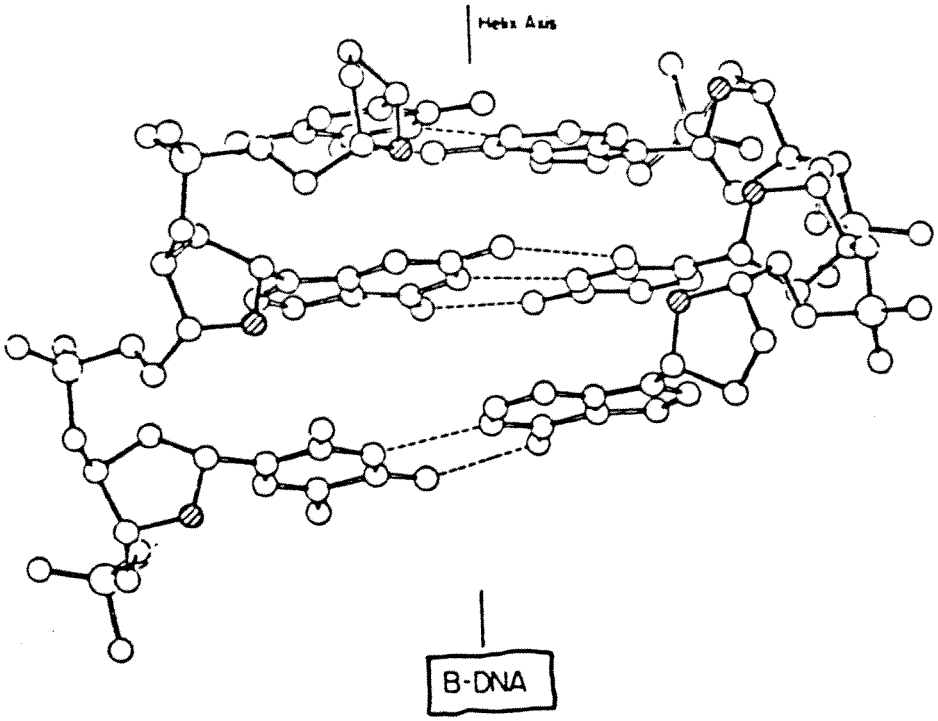

Figure 14. A double helical segment of B-DNA showing three base pairs and base stacking.

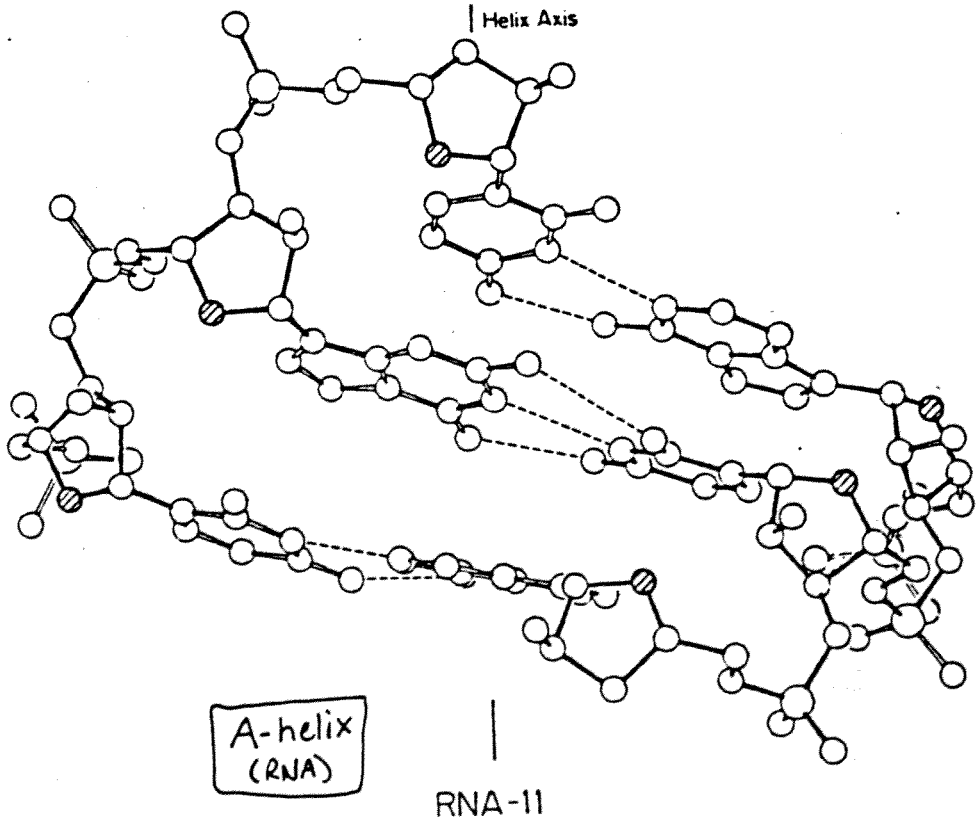

Figure 16. A double helical segment of RNA-11 showing three base pairs and base stacking.

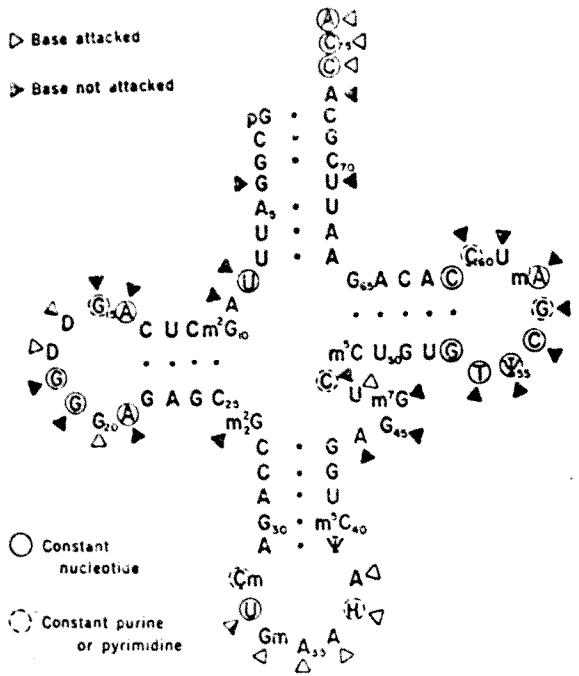

FIG. 9. Summary of the results of the base-specific chemical modification experiments on many D,V$_5$ class tRNAs is shown in relation to the nucleotide sequence of yeast tRNA^{Phe}. H = hypermodified guanosine. The circled bases are invariant, and the dashed circles indicate the semi-invariant bases in all tRNAs participating in peptide elongation (i.e., a G thus marked may be A, a C may be a U in other D,V$_5$-class tRNAs). The accessibility of various bases to chemical modification is indicated by open or filled triangles. The half-filled triangles indicate the bases with possible partial exposure.

I. Conformation of tRNA in Solution and in the Crystal

There is always some doubt as to whether the crystal structure determined is the same as the structure in solution, especially when one considers the molecular contacts necessary to build up the crystal lattice. The solution conformation as measured by circular dichroism (CD) is quite variable depending on the specific solvent conditions (86). However, the interpretation of CD change in terms of the quantitative extent of the change in conformation is difficult at the present time. Overall consistency between the 3-D tRNA structure in the crystal and the structure in aqueous solution as examined by the physical and chemical experiments mentioned above is quite good. Additional evidence for the similarity of the conformations in solution and in the crystal comes from the direct comparison of the fluorescence life-times, in crystal form

and in solution, of the hypermodified base that lies at the 3′ side o the anticodon of yeast tRNA^{Phe}. The fluorescence properties of thi base are very sensitive to the environment, i.e., to the conformatio of the anticodon loop (87, 54). The fluorescence life-time of this bas for tRNA in the orthorhombic crystal is identical with that in the solutio from which these crystals were grown, and very similar to that in th dilute solution of tRNA (88). Thus within the limits of the sensitivit of the method, the conformation of the anticodon loop around this hyper modified base is the same in the crystal and in solution.

In conclusion, one can say that the conformation of *free* tRNA i solution is likely to be almost the same as that found in the crystal, es pecially since about 75% of the crystal volume is occupied by buffer a is the case with an orthorhombic crystal of yeast tRNA^{Phe} (89).

VI. Functional Implications of the 3-D Structure of tRNA

A. Protein-tRNA Recognition

As pointed out in Section II, tRNA goes through many differen recognition processes with various proteins. Some proteins, such a EF-Tu factor and tRNA nucleotidyltransferase, presumably recogniz those features common to all tRNAs, some recognize only certain specifi tRNAs, and others behave in between. The first case is easy to under stand. The proteins in this category probably recognize the commor phosphate-ribose backbone structure (see Section IV, II), or the invar iant and semi-invariant bases (see Fig. 3), or the combination of bot in tRNA.

Recognition of the second type is difficult to predict and is discusse below in terms of the interaction of aminoacyl-tRNA synthetase an its cognate tRNA.

Examination of the 3-D structure of yeast tRNA^{Phe} reveals that mos of the methyl groups in modified nucleosides appear not to be essentia in maintaining the tertiary structure, thus implying a functional role fo them as recognition markers for certain proteins.

B. tRNA-Synthetase Interaction

The fidelity of the genetic information transfer depends primarily on the accuracy in (a) aminoacylation of each tRNA by its cognate aminoacyl-tRNA synthetase (amino-acid:tRNA ligase) and (b) the codon–anticodon interaction. The tRNA–cognate synthetase interaction is likely to involve two types of recognition: a nonspecific recognition

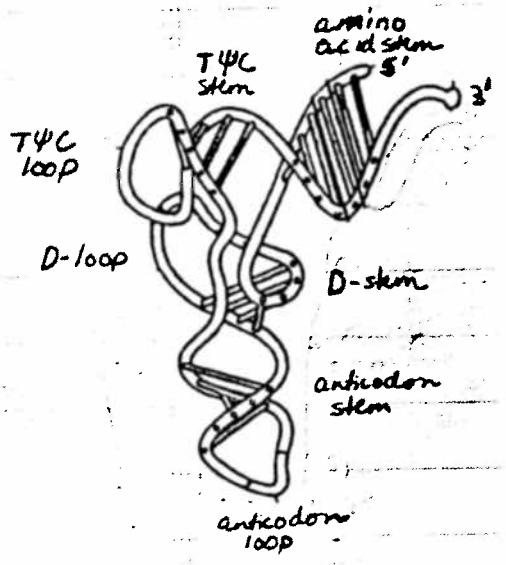

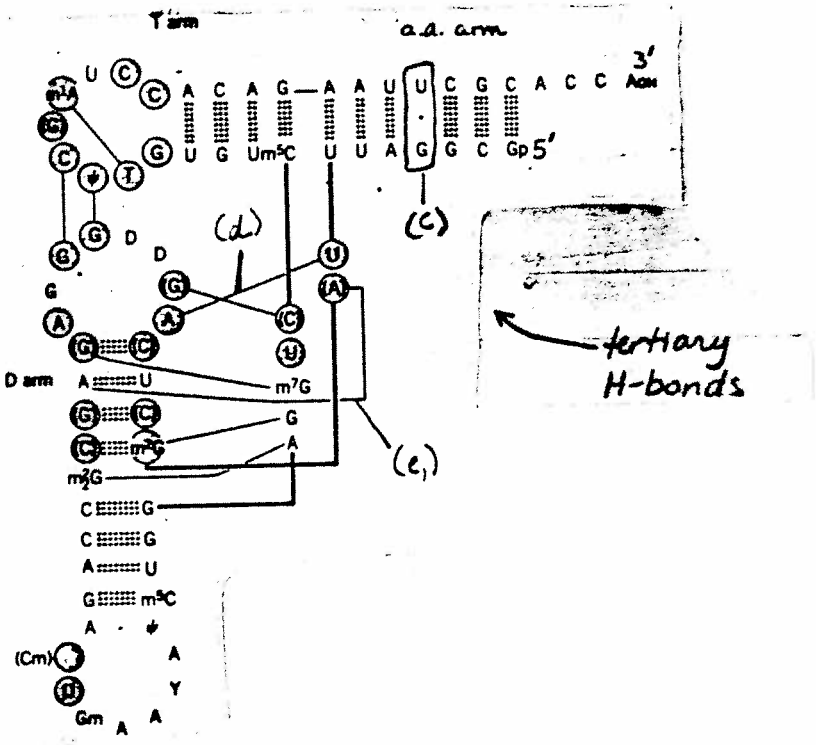

Some tertiary H-Bonds in Yeast tRNA^{phe}

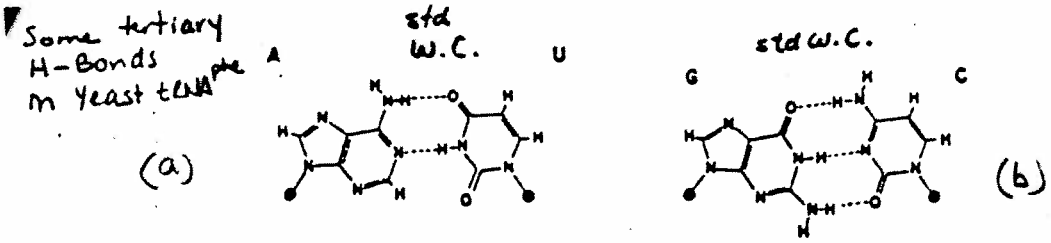

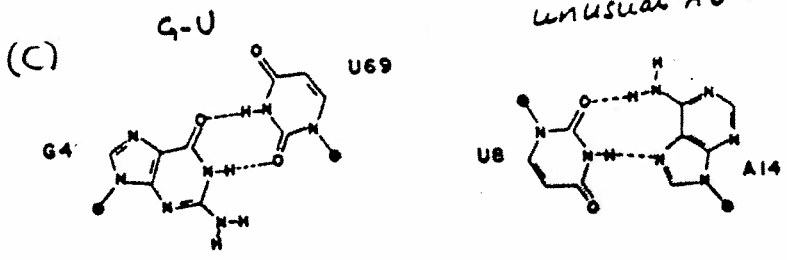

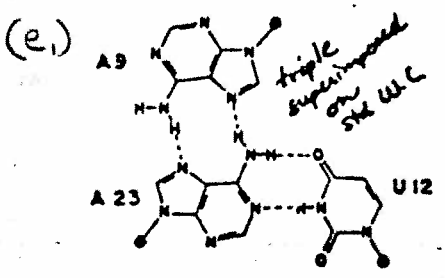

Open access, freely available online

Primer

Pseudoknots: RNA Structures with Diverse Functions

David W. Staple, Samuel E. Butcher*

RNA molecules fulfill a diverse set of biological functions within cells, from the transfer of genetic information from DNA to protein, to enzymatic catalysis. Reflecting this range of roles, simple linear strings of RNA—made up of uracil, guanine, cytosine, and adenine—form a variety of complex three-dimensional structures. Just as proteins form distinct structural motifs such as zinc fingers and beta barrels, certain structures are also commonly adopted by RNA molecules. Among the most prevalent RNA structures is a motif known as the pseudoknot. First recognized in the turnip yellow mosaic virus [1], a pseudoknot is an RNA structure that is minimally composed of two helical segments connected by single-stranded regions or loops (Figure 1). Although several distinct folding topologies of pseudoknots exist, the best characterized is the H type. In the H-type fold, the bases in the loop of a hairpin form intramolecular pairs with bases outside of the stem (Figure 1A and 1B). This causes the formation of a second stem and loop, resulting in a pseudoknot with two stems and two loops (Figure 1C). The two stems are able to stack on top of each other to form a quasi-continuous helix with one continuous and one discontinuous strand. The single-stranded loop regions often interact with the adjacent stems (loop 1–stem 2 or loop 2–stem 1) to form hydrogen bonds and to participate in the overall structure of the molecule. Hence, this relatively simple fold can yield very complex and stable RNA structures. Due to variation of the lengths of the loops and stems, as well as the types of interactions between them, pseudoknots represent a structurally diverse group. It is fitting that they play a variety of diverse roles in biology. These roles include forming the catalytic core of various ribozymes [2,3], self-splicing introns [4], and telomerase [5]. Additionally, pseudoknots play critical roles in altering gene expression by inducing ribosomal frameshifting in many viruses [6–9].

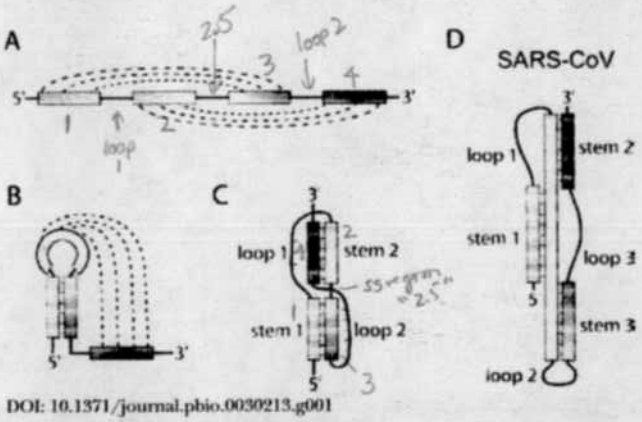

DOI: 10.1371/journal.pbio.0030213.g001

Figure 1. RNA Pseudoknot Architecture
(A) Linear arrangement of base-pairing elements within an H-type RNA pseudoknot. Base pairing is indicated with dashed lines.
(B) Formation of initial hairpin within pseudoknot sequence. Base pairings from loop to bases outside the hairpin are indicated with dashed lines.
(C) Classic H-type pseudoknot fold.
(D) Three-stemmed RNA pseudoknot fold from SARS-CoV.

Catalytically Active Pseudoknots

Hepatitis delta virus (HDV) is a satellite virus of hepatitis B virus. Infection of humans by both HDV and hepatitis B virus is generally more severe than a hepatitis B virus infection alone [10]. HDV has a circular genome that is replicated by the host RNA polymerase II through a double-rolling-circle mechanism. This mechanism produces long strands of RNA that must be processed into unit lengths for viral replication. The processing of the viral RNA is achieved by the self-cleaving HDV ribozyme encoded in the RNA [11]. The HDV ribozyme folds into a double-pseudoknot conformation and self-cleaves, producing single-genome-length HDV RNAs. The HDV ribozyme is the fastest-known naturally occurring self-cleaving ribozyme, with a cleavage rate greater than one per second, and is active in vitro in the absence of any proteins [12]. The HDV ribozyme consists of five helical segments that form two coaxial stacks of two (stems P2 and P3) and three (stems P1, P1.1, and P4) helices each (Figure 2A) [3,13]. Two pseudoknots are formed, each with one helix from each coaxial stack (stems P1 and P2, and stems P3 and P1.1). These two pseudoknots stack on top of each other, forming a nested double-pseudoknot conformation [13].

The removal of introns from pre–messenger RNA (pre-mRNA) is fundamentally important for eukaryotic life. Most introns are removed by a ribonucleoprotein complex called the spliceosome. A subset of introns are self-cleaving, catalyzing their own removal from pre-mRNA without the aid of proteins [14]. One such class of introns are the group I

Primers provide a concise introduction into an important aspect of biology highlighted by a current *PLoS Biology* research article.

Citation: Staple DW, Butcher SE (2005) Pseudoknots: RNA structures with diverse functions. PLoS Biol 3(6): e213.

Abbreviations: HDV, hepatitis delta virus; MMTV, mouse mammary tumor virus; mRNA, messenger RNA; NMR, nuclear magnetic resonance; SARS-CoV, severe acute respiratory syndrome coronavirus

David W. Staple and Samuel E. Butcher are in the Department of Biochemistry at the University of Wisconsin-Madison, Madison, Wisconsin, United States of America.

*To whom correspondence should be addressed. E-mail: butcher@nmrfam.wisc.edu

DOI: 10.1371/journal.pbio.0030213

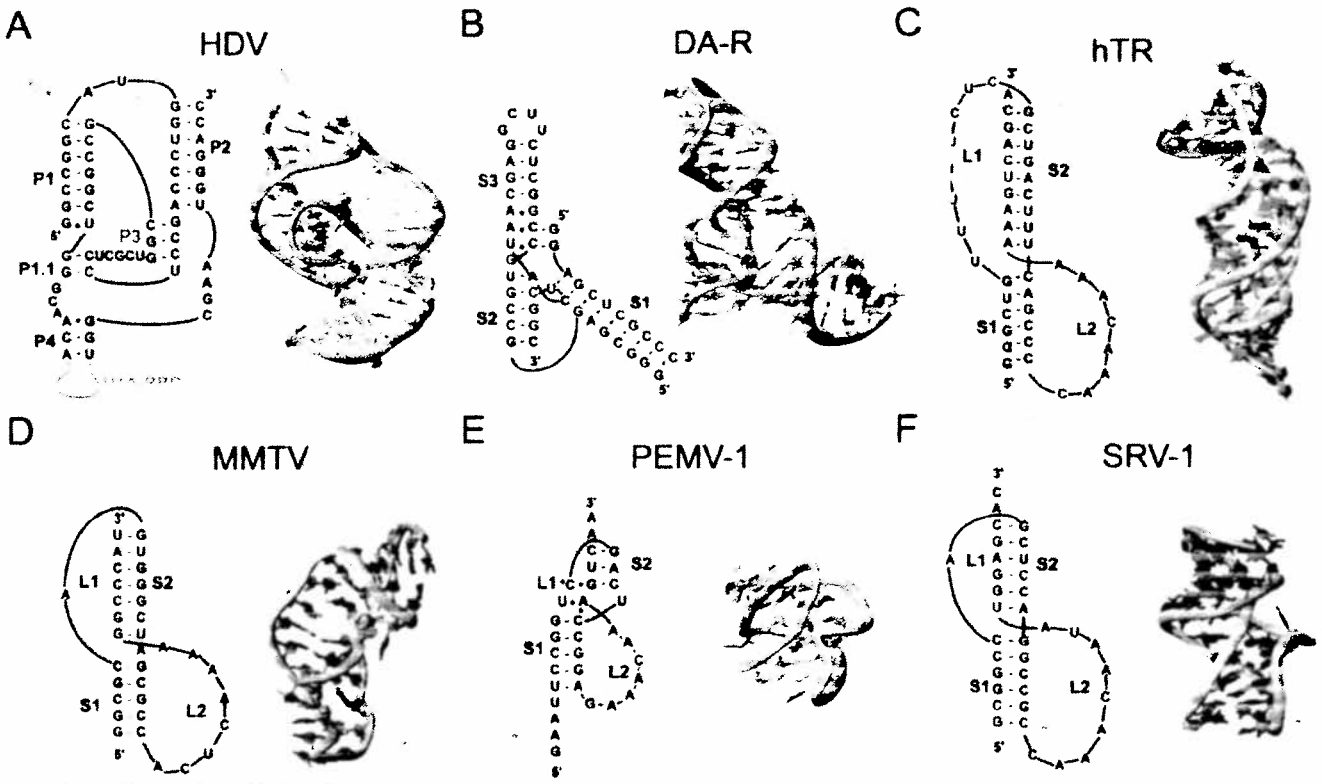

DOI: 10.1371/journal.pbio.0030213.g002

Figure 2. Sequences and Structures of RNA Pseudoknots

Stems and loops are numbered sequentially, unless otherwise noted. Structure coordinates were obtained from the Protein Data Bank (http://www.rcsb.org), and structural representations were produced using MOLMOL software.

(A) HDV (1SJ3). Numbering of stems reflects standard nomenclature for HDV. The U1A RNA binding domain is colored gray and is not included in the three-dimensional structure.

(B) Diels-Alder ribozyme (DA-R) (1YLS).

(C) Human telomerase (hTR) (1YMO).

(D) MMTV (1RNK).

(E) Pea enation mosaic virus RNA1 (PEMV-1) (1KPZ).

(F) Simian retrovirus 1 (SRV-1) (1E95).

self-splicing introns, with the most well-studied example being from the ciliate *Tetrahymena*. The structure of this ribozyme is made up of three helical domains, with many tertiary contacts between the domains [15]. The only portion of the RNA that spans all three helical domains is a pseudoknot belt that wraps around the molecule, base-pairing with all three helices [15]. The pseudoknot establishes the catalytic core of the group I self-splicing introns.

Naturally occurring ribozymes appear to perform mainly hydrolysis and transesterification reactions [16]; however, in vitro selection has yielded RNAs capable of performing a wide variety of enzymatic reactions [17]. Recently the structure of an RNA capable of catalyzing carbon–carbon bond formation by the Diels-Alder reaction was solved (Figure 2B) [18]. The RNA adopts a -shaped fold of its three helices in which stems 2 and 3 stack coaxially, with stem 1 abutting the active site, forming a pocket precisely complementary to the reaction product. The 5′ end of the RNA bridges helical stems 3 and 1, generating a complex nested pseudoknot topology. Although conformationally distinct from the HDV ribozyme [3], it is worthwhile to note that they are two of the fastest-known ribozymes, and both utilize a nested pseudoknot architecture [18].

Chromosomes possess protective ends known as telomeres to protect themselves from degradation due to successive rounds of DNA synthesis. Telomerase, the ribonucleoprotein complex responsible for the maintenance of the telomere ends [19], is upregulated in most cancers [20] and might play a role in aging [21]. Human telomerase is made up of a 451-nucleotide RNA, a reverse transcriptase, and other proteins [22]. At the 5′ end of the RNA is a highly conserved pseudoknot, required for activity, which lies at the core of telomerase. The structure of the human telomerase pseudoknot reveals a classic H-type pseudoknot fold with a slight bend between the stems (Figure 2C) [5]. A triple-helix structure flanks the junction of the helices and extends into each stem. Mutations within the telomerase pseudoknot have been directly linked to the diseases autosomal dyskeratosis congenita [21] and aplastic anemia [23].

Frameshift-Inducing Pseudoknots

Not all pseudoknots with biological functions are catalytically active. In fact, one of the most common functions of pseudoknots is to induce ribosomes to slip into alternative reading frames, otherwise known as frameshifting. Ribosomes typically translate mRNA without shifting the translational

B-form polydApolydT selectivity by a cubane-like europium-L-aspartic acid complex". *Biophysical Journal* **90** (9): 3203–3207. doi:10.1529/biophysj.105.078402. PMC 1432110. PMID 16473901. http://www.biophysj.org/cgi/content/full/90/9/3203.

7. ^ Ho PS, Ellison MJ, Quigley GJ, Rich A (1986). "A computer aided thermodynamic approach for predicting the formation of Z-DNA in naturally occurring sequences". *EMBO Journal* **5** (10): 2737–2744. PMC 1167176. PMID 3780676. http://www.pubmedcentral.nih.gov/articlerender.fcgi?tool=pmcentrez&artid=1167176.
8. ^ *a b* Champ PC, Maurice S, Vargason JM, Camp T, Ho PS (2004). "Distributions of Z-DNA and nuclear factor I in human chromosome 22: a model for coupled transcriptional regulation". *Nucleic Acids Res.* **32** (22): 6501–6510. doi:10.1093/nar/gkh988. PMC 545456. PMID 15598822. http://nar.oxfordjournals.org/cgi/pmidlookup?view=long&pmid=15598822.
9. ^ Rich A, Zhang S (2003). "Timeline: Z-DNA: the long road to biological function". *Nature Review Genetics* **4** (7): 566–572. doi:10.1038/nrg1115. PMID 12838348.
10. ^ Halber D (1999-09-11). "Scientists observe biological activities of 'left-handed' DNA". MIT News Office. http://web.mit.edu/newsoffice/1999/zdna-0911.html. Retrieved 2008-09-29.
11. ^ Kim YG, Muralinath M, Brandt T, Pearcy M, Hauns K, Lowenhaupt K, Jacobs BL, Rich A (2003). "A role for Z-DNA binding in vaccinia virus pathogenesis". *Proc Natl Acad Sci USA* **100** (12): 6974–6979. doi:10.1073/pnas.0431131100. PMC 165815. PMID 12777633. http://www.pubmedcentral.nih.gov/articlerender.fcgi?tool=pmcentrez&artid=165815.
12. ^ Kim YG, Lowenhaupt K, Oh DB, Kim KK, Rich A (2004). "Evidence that vaccinia virulence factor E3L binds to Z-DNA in vivo: Implications for development of a therapy for poxvirus infection". *Proc Natl Acad Sci USA* **101** (6): 1514–1518. doi:10.1073/pnas.0308260100. PMC 341766. PMID 14757814. http://www.pubmedcentral.nih.gov/articlerender.fcgi?tool=pmcentrez&artid=341766.
13. ^ Sinden, Richard R (1994-01-15). *DNA structure and function* (1st ed.). Academic Press. pp. 398. ISBN 0-12-645750-6.
14. ^ Rich A, Norheim A, Wang AHJ (1984). "The chemistry and biology of left-handed Z-DNA". *Annual Review of Biochemistry* **53** (1): 791–846. doi:10.1146/annurev.bi.53.070184.004043. PMID 6383204.
15. ^ Ho PS (1994-09-27). "The non-B-DNA structure of d(CA/TG)n does not differ from that of Z-DNA". *Proc Natl Acad Sci USA* **91** (20): 9549–9553. doi:10.1073/pnas.91.20.9549. PMC 44850. PMID 7937803. http://www.pubmedcentral.nih.gov/articlerender.fcgi?tool=pmcentrez&artid=44850.

External links

- ZHunt Online Server

Retrieved from "http://en.wikipedia.org/wiki/Z-DNA"
Categories: DNA